QUANTUM CHEMICAL INVESTIGATION OF *trans*- and *cis*-ISOMERS OF FLUPENTIXOL AS A NANO-DRUG**

Z. A. Saleh, S. B. Novir*, E. Balali

Department of Pharmaceutical Chemistry, Faculty of Pharmaceutical Chemistry, Tehran Medical Sciences, Islamic Azad University, Tehran, Iran;
e-mail: samaneh_bn83@yahoo.com, sa_bagheri@chem.iust.ac.ir

*Geometrical structure, electronic and optical properties, electronic absorption spectra, vibrational frequencies, natural charge distribution, thermodynamic properties, and MEP analysis of trans- and cis-structures of Flupentixol have been investigated using DFT and TDDFT methods with the B3LYP hybrid functional and 6-311+G** basis set. The results of calculation of the quantum properties verify the greater activity of the cis structure of this drug.*

Keywords: *Flupentixol, schizophrenia, density functional theory, electronic properties.*

КВАНТОВО-ХИМИЧЕСКОЕ ИССЛЕДОВАНИЕ *транс*- и *цис*-ИЗОМЕРОВ ФЛУПЕНТИКСОЛА КАК НАНОПРЕПАРАТА

Z. A. Saleh, S. B. Novir*, E. Balali

УДК 535.34:615.012.8

Исламский университет Азада, Тегеран, Иран;
e-mail: samaneh_bn83@yahoo.com, sa_bagheri@chem.iust.ac.ir

(Поступила 22 сентября 2017)

*С использованием DFT и TDDFT методов с гибридным функционалом B3LYP и базисным набором 6-311+G** исследованы геометрическая структура, электронные и оптические свойства, электронные спектры поглощения, частоты колебаний, естественное распределение заряда, термодинамические свойства, а также проведен анализ молекулярного электростатического потенциала транс- и цис-структур препарата флупентиксол. Результаты расчетов квантовых свойств подтверждают высокую активность цис-структуры этого препарата.*

***Ключевые слова*:** *флупентиксол, шизофрения, теория функционала плотности, электронные свойства.*

Introduction. Flupentixol (FLP) (trading name Depixol or Fluanxol, IUPAC name (*EZ*)-2-[4-[3-[2-(trifluoromethyl)thioxanthen-9ylidene]propyl]piperazin-1-yl]ethanol) is used to treat schizophrenia and depression. It is an antipsychotic drug of the thioxanthene group. Medications of the thioxanthene category are effective in the treatment of schizophrenia, idiopathic psychotic diseases, organic psychoses, and other neuropsychiatric illnesses [1–5]. A higher dose of Flupentixol is used for the therapy of schizophrenia, while a lower dose may be used in severe depression accompanied by psychotic symptoms [4, 5]. Thioxanthene drugs may be used in other fields, namely as an antinausea, antiemetic, antihistamine, sedative, or general anesthetic drug [1, 5]. Flupentixol is used as dihydrochloride in the form of drops and tablets, or as decanoid acid ester for injections [3, 6]. The chemical structure of Flupentixol, which consists of the thioxanthene ring and a side chain connected to the thioxanthene ring by a C=C double bond, is shown in Fig. 1. As seen in Fig. 1, the presence of the C=C double bond in the structure of Flupentixol demonstrates that Flupentixol has

** Full text is published in JAS V. 86, No. 6 (https://www.springer.com/journal/10812) and in electronic version of ZhPS V. 86, No. 6 (http://www.elibrary.ru/title_about.asp?id=7318; sales@elibrary.ru).

two different *trans*(*E*)- and *cis*(*Z*)-geometric isomers. Only the *cis*-isomer (*Z*) is known as pharmacological active, while the *trans*-isomer (*E*) is actually inactive. The tablets or drops form of Flupentixol are a mixture of the *cis*(*Z*)- (active) and the *trans*(*E*)- (inactive) isomers, but only the *cis*-isomer (*Z*) has been used for injections [3, 5–7]. The possibility of *trans*(*E*)/*cis*(*Z*) isomerization around the C=C double bond in Flupentixol can affect its biologically properties. Therefore, the *cis*/*trans*-isomerization of Flupentixol is of great interest from the biological point of view [8]. It should be noted that changes in molecular structure due to the influence of ultraviolet-visible light may change the biological activity of drugs [5, 8, 9]. Quantum chemical methods can be an appropriate tool for understanding the correlation between the molecular structures of drugs and their pharmacological activity. Some experimental and theoretical investigations of the molecular and spectroscopic properties of antidepressant drugs are known [10–18], but Flupentixol medication has not yet been investigated by computational methods. In this study, both *trans*- and *cis*-structures of Flupentixol were studied with quantum chemical computational methods. The correlation between the biological properties of isomers and their calculated quantum parameters was established. The main objective of this paper is to study the molecular structure and nonlinear optical properties such as polarizability and hyperpolarizability, electronic absorption spectra, thermodynamic parameters, and other molecular properties on the basis of the density functional theory (DFT) and the time-dependent DFT (TDDFT) methods.

Computational methods. All quantum chemical calculations were performed with the GAMESS package [19]. The solvent effects (in this study water is defined as solvent) were studied with the conductor polarizable continuum model (CPCM) [20–22]. The *trans*- and *cis*-molecular structures of Flupentixol were optimized using DFT [23] with the B3LYP functional [24–26] and 6-311+G** basis set. The optimized geometries were used in the vibrational frequency calculations to confirm that the structures reached a stationary point with minimum energy and no imaginary frequencies, and to estimate the thermodynamic parameters and nonlinear optical properties (NLO) such as polarizability and hyperpolarizability. The excitation energies, maximum absorbances (λ_{max}), oscillator strengths (*f*), and absorption spectra of two isomers of Flupentixol were calculated with the time-dependent DFT (TDDFT) method at B3LYP/6-311+G** for the lowest 30 singlet-singlet transitions based on the optimized ground state geometries. Natural bond orbital (NBO) calculations of two isomers of Flupentixol were carried out at the same level on the optimized structures. Also, the reactive sites of this drug, evaluated with the molecular electrostatic potential (MEP), were investigated by the B3LYP/6-311+G** method.

Results and discussion. *Geometrical structures.* The optimized geometries of the two structures are shown in Fig. 1. The selected optimized bond lengths, bond angles, and dihedral angles of the two structures are listed in Table 1. These data show that the optimization in the solvent phase does not change the structural parameters. All the CC lengths in the two phenyl rings are between the distance of a single bond and a double bond, which shows that there are resonance bonds in both rings of the *cis*- and *trans*-structures. The aromaticity of the benzene rings, because of the substitutions, is distorted from the hexagonal structure. The difference in bond lengths between C18-C20 and C25-C27 is 0.019 and 0.020 Å in the *trans*- and

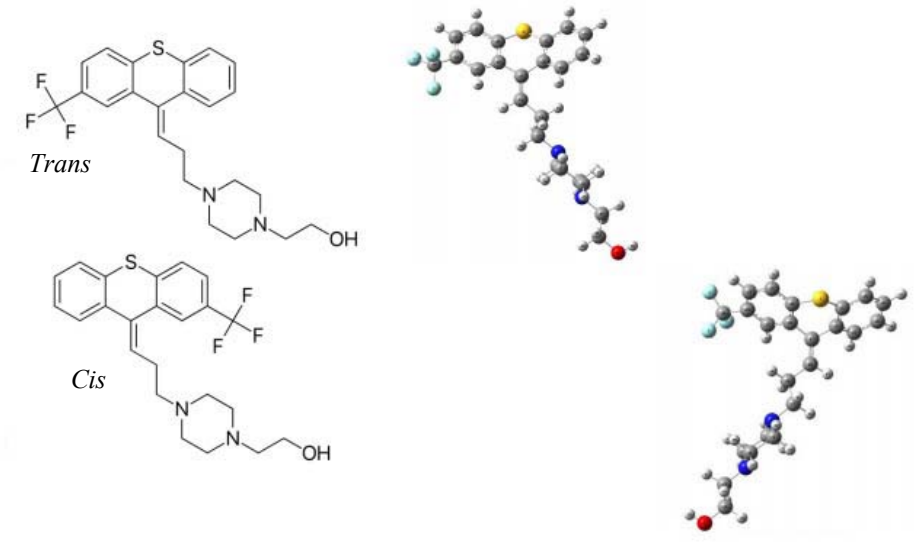

Fig. 1. Molecular structure and optimized molecular structure of *trans*- and *cis*-Flupentixol at the B3LYP/6-311+G** level of theory.

cis-structures, respectively. Also, the difference in bond lengths between C21-C19 and C23-C28 is 0.016and 0.015 Å in the *trans*- and *cis*-structures, respectively. The difference in bond angles between C25-C20-C18 and C20-C18-C22 is 2.7° and 3° in the *trans*- and *cis*-structures, respectively. Also, the difference in bond angles between C28-C23-C19 and C23-C19-C21 is 3.6° and 3.3° in the *trans*- and *cis*-structures, respectively. In both *trans*- and *cis*-isomers of the molecule, the C19–C21 and C18-C20 bond lengths are slightly larger than the other CC bond lengths of the phenyl rings. The S1-C20 and S1-C21 bond lengths in the middle ring are larger than the other bond lengths in this ring. The C14-C12, C13-C15, C8-C10, and C11-C9 bond lengths are longer than the other CC bond lengths in the molecule. As seen in Table 1, the C19-C17-C16 bond angle of the trans structure is slightly larger than that of the cis structure, and the C18-C17-C16 bond angle in the trans structure is slightly smaller than that of the cis structure. The other bond lengths and bond angles in the trans and cis structures are almost close to each other. The calculated dihedral angles C18-C17-C16-C14, C19-C17-C16-C14, C22-C18-C17-C16, C23-C19-C17-C16, and C17-C16-C14-C12 in the solvent phase, corresponding to the *trans*- and *cis*-structures, are 175.1, –2.4, 42.5, –45.1, –136.4 and –2.5, 175.3, –45.3, 42.4, –138.1°, respectively. The dihedral angles are significantly affected by the isomerization of Flupentixol from the trans to cis isomer.

TABLE 1. Selected Bond Lengths (Å), Bond Angles (deg.) and Dihedral Angles (deg.) of the *trans*- and *cis*-Structures of Flupentixol at the B3LYP/6 311+G** Level of Theory

Bond	*trans* gas/water	*cis* gas/water	Bond	*trans* gas/water	*cis* gas/water
Bond lengths			*Bond angles*		
S1-C20	1.777/1.779	1.777/1.778	C22-C24-C27	120.2/120.4	120.2/120.4
S1-C21	1.783/1.786	1.784/1.786	C24-C27-C25	119.5/119.4	119.4/119.4
C21-C19	1.406/1.406	1.404/1.405	C27-C25-C20	120.3/120.2	120.3/120.2
C19-C23	1.402/1.403	1.401/1.402	C25-C20-C18	120.7/120.8	120.7/120.9
C23-C28	1.390/1.391	1.390/1.391	C20-C18-C22	118.1/118.1	117.9/117.9
C28-C29	1.394/1.395	1.394/1.395	C18-C22-C24	121.1/120.9	121.1/120.9
C29-C26	1.390/1.391	1.390/1.391	C30-C24-C22	119.6/119.5	119.6/119.7
C26-C21	1.396/1.397	1.396/1.397	C30-C24-C27	120.1/119.9	120.0/119.8
C19-C17	1.484/1.484	1.486/1.486	C17-C18-C20	120.1/121.2	120.0/120.2
C17-C18	1.486/1.487	1.484/1.484	C18-C20-S1	120.8/120.7	120.8/120.7
C18-C20	1.406/1.407	1.407/1.407	C20-S1-C21	100.0/100.1	100.0/100.1
C20-C25	1.397/1.398	1.398/1.398	S1-C21-C19	120.8/120.7	120.7/120.7
C25-C27	1.388/1.388	1.387/1.387	C21-C19-C17	120.0/120.1	120.1/120.1
C27-C24	1.395/1.396	1.395/1.396	C19-C17-C18	115.4/115.4	115.4/115.4
C24-C22	1.392/1.393	1.392/1.392	C19-C21-C26	120.9/121.1	120.9/121.1
C22-C18	1.398/1.399	1.399/1.400	C21-C26-C29	120.0/119.8	119.9/119.8
C24-C30	1.502/1.499	1.502/1.499	C26-C29-C28	119.8/119.8	119.8/119.8
C30-F2	1.352/1.354	1.352/1.354	C29-C28-C23	119.9/119.9	119.9/119.9
C30-F3	1.353/1.354	1.353/1.354	C28-C23-C19	121.3/121.3	121.2/121.2
C30-F4	1.359/1.364	1.359/1.364	C23-C19-C21	117.8/117.7	117.9/117.9
C17-C16	1.347/1.347	1.347/1.347	C19-C17-C16	124.5/124.5	120.2/120.4
C16-C14	1.501/1.501	1.500/1.501	C18-C17-C16	119.9/119.9	124.3/124.0
C14-C12	1.538/1.538	1.539/1.538	C17-C16-C14	128.7/128.6	129.0/128.5
C12-N6	1.460/1.463	1.460/1.462	F2-C30-F3	107.0/106.8	107.1/106.8
N6-C8	1.462/1.465	1.462/1.465	F2-C30-F4	106.4/106.0	106.3/105.9
C8-C10	1.526/1.525	1.525/1.525	F3-C30-F4	106.3/105.9	106.3/106.0
C10-N7	1.462/1.466	1.463/1.466	*Dihedral angles*		
N7-C11	1.463/1.465	1.463/1.466	C18-C17-C16-C14	174.7/175.1	–1.5/–2.5
C11-C9	1.524/1.524	1.525/1.524	C19-C17-C16-C14	–2.5/–2.4	175.7/175.3
C9-N6	1.463/1.465	1.463/1.465	C22-C18-C17-C16	42.7/42.5	–45.9/–45.3
N7-C13	1.459/1.463	1.459/1.463	C23-C19-C17-C16	–45.4/–45.1	43.2/42.4
C13-C15	1.531/1.530	1.531/1.530	C17-C16-C14-C12	–135.4/–136.4	–131.9/–138.1
C15-O5	1.427/1.433	1.427/1.433			

Energy levels. The E_{HOMO}, E_{LUMO}, HLG ($E_{LUMO} - E_{HOMO}$), total molecular energies, and relative energies for the *trans*- and *cis*-structures of Flupentixol are shown in Table 2. The computed HOMO energy levels of the *trans*- and *cis*-structures in the gas phase (water solvent) are located at –6.099 and –6.093 eV (–6.068 and –6.062 eV), and their corresponding LUMO energy levels are located at –1.651 and –1.667 eV (–1.575 and –1.613 eV), respectively. In the presence of both gas and solvent phases, the HOMO energy levels of the trans structure of Flupentixol are lower than the HOMO energy level of the *cis*-structure, while, the LUMO energy levels of the trans structure are higher than the *cis*-structures. Therefore, the HLG of the *trans*-structure of Flupentixol is greater than the HLG of the *cis*-structure. The relative energies of the structures in both gas and solvent phases show that the *cis*-structure of Flupentixol is more stable than the *trans*-structure by 0.001 and 0.009 eV, in the gaseous and water phases, respectively. The relative energy in the solvent phase is higher than that in the gaseous phase. This means that the stability of the *cis*-structure relative to the *trans*-structure in the solvent phase is greater than in the gaseous phase.

TABLE 2. E_{HOMO} (eV), E_{LUMO} (eV), HLG (eV), Total Energy (eV), and Relative Energy $\Delta E = E_{cis} - E_{trans}$ (eV) of the *trans*- and *cis*-structures of Flupentixol using the B3LYP/6-311+G** Method in the Gaseous and Water Phases

Phase	Flupentixol	E_{HOMO}	E_{LUMO}	HLG	Total energy	ΔE
Gas	*trans*	–6.099	–1.651	4.448	–48273.067	–0.001
	cis	–6.093	–1.667	4.426	–48273.068	
Water	*trans*	–6.068	–1.575	4.493	–48283.477	–0.009
	cis	–6.062	–1.613	4.448	–48283.486	

Electronic absorption spectra. The electronic absorption spectra of *trans*- and *cis*-structures of flupentixol were evaluated by the time-dependent DFT (TDDFT) method at the B3LYP/6-311+G** level of theory in both gaseous and water phases based on the optimized ground state geometries of the molecule. The excitation energies, maximum wavelengths (λ_{max}), oscillator strengths (*f*), main transition, and electronic transition configurations of the *trans*- and *cis*-isomers of Flupentixol in both gaseous and solvent phases and the calculated UV-Vis absorption spectra of both structures of Flupentixol in the two phases with a Gaussian line broadening of 0.333 eV are shown in Table 3 and Fig. 2, respectively. The maximum absorption wavelengths (λ_{max}) of the *trans*- and *cis*-isomers of Flupentixol in the gaseous phase are predicted at 229 nm with an oscillator strength $f = 0.280$ and at 230 nm with the oscillator strength $f = 0.288$, respectively. Also, the λ_{max} of *trans*- and *cis*-configurations of this compound in the water phase, carried out with the CPCM model in the TDDFT calculations, are predicted at 232 nm with the oscillator strength $f = 0.331$ and 231 nm with the oscillator strength $f = 0.316$, respectively. The presence of water as solvent shifts the absorption bands of the *trans*- and *cis*-structures of flupentixol toward slightly longer wavelengths and larger oscillator strengths. With increasing the solvent polarity, the energy of the excited state is lowered more than that of the ground state. Therefore, the λ_{max} of both structures of Flupentixol has a slight red shift by the solvent effects [27]. The maximum absorption wavelengths are associated with the HOMO–3→LUMO+2 transitions. Owing to this, the highest electronic transitions related to the λ_{max} are associated with orbitals 111 and 117. Since orbital 114 is defined as HOMO and orbital 115 is defined as LUMO, the highest electronic transitions related to λ_{max} are associated to HOMO–3→LUMO+2. The percentages of this electronic transition for the *cis*-structure are higher than the *trans*-structure, in both phases.

TABLE 3. Calculated Excitation Energies (E_{exc}, eV), Maximum Wavelengths (λ_{max}, nm), Oscillator Strengths (*f*), Main Transition, Electronic Transition Configurations, E_{HOMO-3} and E_{LUMO+2} of the *trans*- and *cis*-Structures of Flupentixol, Using the TDDFT-B3LYP/6-311+G** Method in Both Gaseous and Solvent Phases

Phase	Flupentixol	E_{exc}	λ_{max}	*f*	Main transition	E_{HOMO-3}	E_{LUMO+2}
Gas	*trans*	5.394	229	0.280	H–3→L+2 (29.82 %)	–6.93	–0.976
	cis	5.388	230	0.288	H–3→L+2 (49.95 %)	–6.90	–0.935
Water	*trans*	5.342	232	0.331	H–3→L+2 (38.82 %)	–6.850	–0.914
	cis	5.344	231	0.316	H–3→L+2 (39.09 %)	–6.829	–0.883

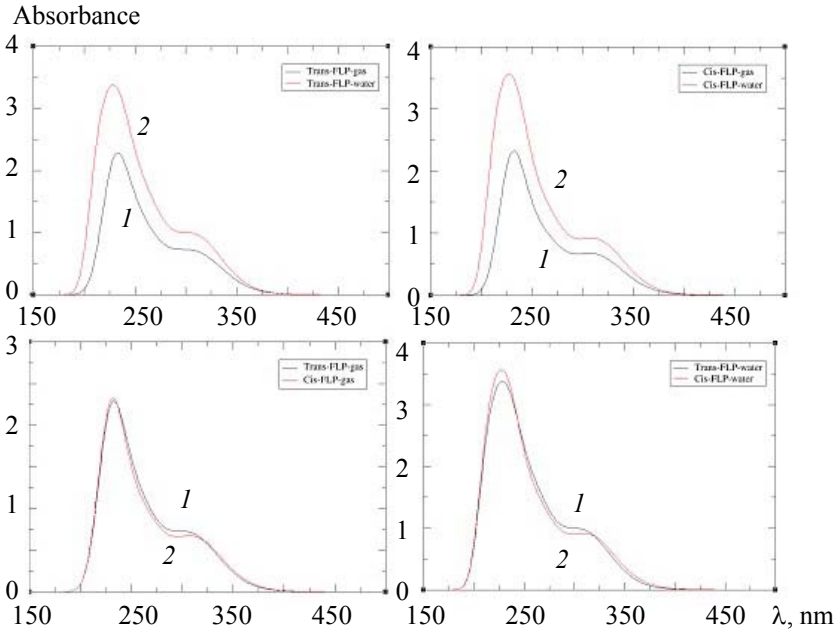

Fig. 2. Electronic absorption spectra of *trans*- (1) and *cis*-Flupentixol (2) in the gaseous phase and solvent (water); calculations made by the TDDFT method using the B3LYP/6-311+G** level of theory.

The frontier molecular orbitals of the *trans*- and *cis*-structures of Flupentixol in the solvent phase (Fig. 3) show that for this compound the frontier molecular orbitals are generally composed of *p* atomic orbitals. Thus, these electronic transitions correspond to the $\pi \rightarrow \pi^*$ transition. These results are almost in qualitative agreement with the experimental results [4]. We cannot obtain exact quantitative results from the TDDFT calculations because there is a small difference between the TDDFT calculations and the experimental results due to the difference between the DFT exchange and the correlation function and the computational model of the solvent effects [28–31]. The results of the TDDFT calculations show that the maximum absorption bands and oscillator strengths of the *cis*-structure of Flupentixol are almost higher than those of the *trans*-structure. Consequently, the *cis*-structure of Flupentixol shows the best absorption properties. The improved properties of the *cis*-structure of Flupentixol can explain its wider application as a medicine.

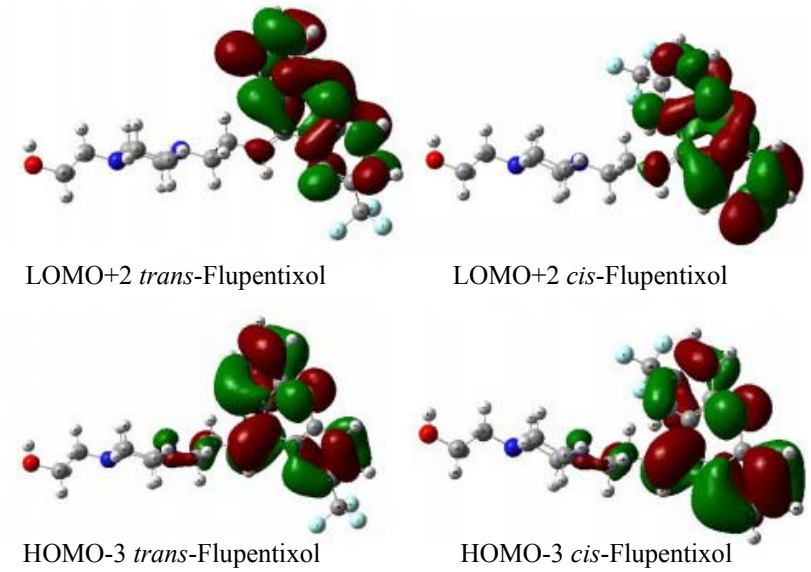

Fig. 3. HOMO-3 and LUMO+2 plots of *trans*- and *cis*-Flupentixol computed at the B3LYP/6-311+G** level in the solvent phase.

Nonlinear optical properties and other molecular properties. The nonlinear optical (NLO) properties (total static dipole moment (μ), mean polarizability (α), anisotropy of polarizability (Δα), and first-order hyperpolarizability (β)) were investigated. The dipole moment can be used as a descriptor to demonstrate the charge transfer within the molecule [32, 33]. Polarizabilities and hyperpolarizabilities are quantities that characterize the reaction of a molecule to an applied electric field [32, 34, 35]. In order to investigate the NLO properties, HLG, and chemical reactivity descriptors such as the electronegativity (χ), chemical hardness (η) and softness (σ), chemical potential (ρ), and electrophilicity index (ω) of the molecule, the equations based on Koopman's theorem [36, 37] were used.

Electronegativity (χ), which is a measure of the power of an atom or a group of atoms to attract electrons [38, 39], can be calculated from the HOMO and LUMO energy level by the equation [32, 35]

$$\chi = (-1/2)(E_{HOMO} + E_{LUMO}). \quad (1)$$

The stability and reactivity of a molecule is related to its chemical hardness (η), which is a measure of the resistance of a system to charge transfer [32, 35]. This parameter can be calculated from the equation

$$\eta = (1/2)[IP - EA] \approx (1/2)(E_{LUMO} - E_{HOMO}). \quad (2)$$

On the basis of Koopman's theorem $IP \approx E_{HOMO}$ and $EA \approx E_{LUMO}$, where *IP* is the ionization potential and *EA* is the electron affinity [32, 35, 38].

The chemical softness (σ), which characterizes the capacity of a molecule to accept electrons and measures the easiness of charge transfer, can be calculated as the inverse of hardness. The softness, which is related to polarizability, means that hard molecules have low polarizability and soft molecules have high polarizability [32, 38, 40].

The electronic chemical potential (ρ), which is the evasion affinity of an electron from equilibrium, was calculated from the equation [40, 41]

$$\rho = -\chi = (1/2)\,(E_{HOMO} + E_{LUMO}). \quad (3)$$

The electrophilicity index (ω), which determines the stabilization energy of the system when it becomes saturated with electrons, can be computed from the electronegativity and chemical hardness using the formula [32, 40, 42]

$$\omega = \chi^2/2\eta. \quad (4)$$

All the parameters above for both *trans*- and *cis*-structures of Flupentixol in the gaseous and solvent phases are calculated with the B3LYP/6-311+G** method and presented in Table 4. According to Table 4, the dipole moments μ, polarizability α, anisotropy of polarizability Δα, and the total first-order hyperpolarizability β_{tot} of *cis*-Flupentixol are higher than those of *trans*-Flupentixol in both gaseous and solvent phases, and the values of μ, α, and β_{tot} in the solvent phase are higher than those in the gaseous phase. The higher dipole moment, polarizability, and hyperpolarizability shows that *cis*-structure of Flupentixol has better NLO properties than the *trans*-stucture. A molecule with the higher dipole moment has stronger intermolecular interactions [32]. From these values we can conclude that the *cis*-structure of Flupentixol, used as a biologically active molecule, is a better NLO molecule than the *trans*-structure. The chemical hardness of these molecules, related to the HLG of these structures, determines the charge transfer and the reactivity of the molecule. Soft molecules with smaller HLG will be more reactive than hard molecules with larger HLG [32, 40, 41, 43]. The chemical hardness of the *trans*-structure of Flupentixol in both gaseous and solvent phases is higher than that of the *cis*-structure. This means that the *trans*-structure is harder than the *cis*-structure, and the chemical softness of the *cis*-structure is higher than that of the *trans*-structure. Therefore, the charge transfer and reactivity of *cis*-Flupentixol is higher than those of *trans*-Flupentixol. According to the results, there is a reverse correlation between the polarizability values and the chemical hardness (η) of the molecule. The *cis*-structure of Flupentixol with the smaller chemical hardness (η) shows a higher λ_{max} and a larger polarizability and hyperpolarizability than the *trans*-structure. The reduced chemical hardness demonstrates that the electron density is more simply influenced and the molecule could be more reactive. The enhanced polarizabilities increase the distortion of the electron cloud by an electric field to the acceptor group and cause higher intramolecular charge transfer capability. Consequently, the smaller chemical hardness means higher polarizability and hyperpolarizability [27, 43]. From Table 4 it is clear that the electronegativity of the *trans*- and *cis*-structures of Flupentixol are observed at 3.387 and 3.880 eV in the gaseous phase and at 3.821 and 3.837 eV in the solvent phase, respectively. The electrophilicity index of the *trans*- and *cis*-structures of Flupentixol in the gaseous phase is 3.376 and 3.401 eV, respectively, and this parameter in the solvent phase is observed at 3.251 and 3.310 eV, respectively. Thus, we can conclude that the electro-

negativity, chemical potential, and electrophilicity index of the *cis*-isomer of Flupentixol in both gaseous and solvent phases are larger than those of the *trans*-isomer. This means that *cis*-Flupentixol has better reactivity on the basis of these chemical reactivity descriptors.

TABLE 4. Calculated Dipole Moment (μ, Debye), Isotropic Polarizability (α), Anisotropy of Polarisability (Δα), Total Frst-order Hyperpolarizability (β_{tot}), Chemical Hardness (η), Softness (σ, eV), Electronegativity (χ), Chemical Potential (ρ), and Electrophilicity Index (ω) of the *trans*- and *cis*-Structures of Flupentixol, Using the B3LYP/6-311+G** Method

Phase	Gas		Water	
Flupentixol	*trans*	*cis*	*trans*	*cis*
Dipole moment μ	3.017	3.796	3.661	4.404
α, 10^{-22} esu	0.480	0.481	0.658	0.659
Δα, 10^{-22} esu	0.148	0.172	0.114	0.173
β_{tot}, 10^{-28} esu	0.041	0.047	0.074	0.113
Chemical hardness η	2.224	2.213	2.246	2.224
Chemical softness σ	0.449	0.452	0.445	0.449
Electronegativity χ	3.387	3.880	3.821	3.837
Chemical potential ρ	–3.387	–3.880	–3.821	–3.837
Electrophilicity index ω	3.376	3.401	3.251	3.310

Natural charge distributions and Molecular electrostatic potential (MEP). The natural atomic charges of the *trans*- and *cis*-conformations of Flupentixol in the gaseous and solvent phases show that all H atoms, S, and C30 atoms have positive natural atomic charges, and all carbon atoms, except for the C30 atom, oxygen, nitrogen, and fluorine atoms, have negative atomic charges. The negative atomic charges of O and N atoms, which are known as electronegative atoms, are higher than those of the carbon atoms. The O5 atom shows the highest negative atomic charge, and the C30 atom, which is connected to three F atoms, shows the highest positive atomic charge among all the atoms of the molecule. Also, the H50 atom shows the highest positive atomic charge among all the H atoms. The molecular electrostatic potential (MEP) is an appropriate method to specify three-dimensional charge distributions of molecules. This counter map is very helpful to characterize the reactive sites of molecules in both electrophilic and nucleophilic reactions for investigation of biological systems [32, 44, 45]. The molecular electrostatic potential for both structures of Flupentixol at the B3LYP/6-311+G** optimized structures were calculated and shown in Fig. 4, to characterize the reactive sites of electrophilic and nucleophilic attacks for the *trans*- and *cis*-conformations of the Flupentixol molecule. Generally, the different values of the electrostatic potential are shown by various colors. The order of the potential values is: red < orange < yellow < green < blue. The maximum positive region (the preferred site for the nucleophilic attack) is shown by the blue color. The negative areas of the MEP, associated with electrophilic reactivity, are identified with the red and yellow colors. The preferred site for the electrophilic attack is shown by the red color. The MEP maps of the Flupentixol molecule show that the negative charges are more concentrated around the oxygen atom and fluorine atoms (the red and yellow color). Therefore, these regions of the molecule are suitable regions for electrophilic reactivity. The area near of the O atom with the red color is the preferred site for electrophilic reactions. The greater electronegativity of the oxygen atoms makes them the most reactive parts for electrophilic reactivity in the molecule [32, 44]. The positive region (blue) is distributed over the hydrogen atom connected to the oxygen atom. This region is the preferred site for nucleophilic reactivity. Most regions of the molecule are neither dark blue nor dark red. This means that these regions are almost neutral.

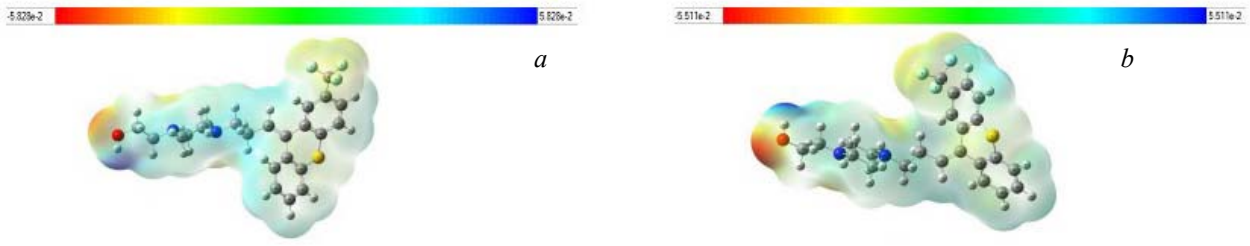

Fig. 4. MEP map of *trans*- (a) and *cis*-Flupentixol (b).

Vibrational spectra. The calculated vibrational frequencies at the B3LYP/6-311+G** level of theory show that the optimized structures of Flupentixol are in stationary points without any imaginary frequency. The obvious vibrational frequencies with the higher IR intensities of two conformations are shown in Table 5. The obvious vibrational frequencies are practically similar for the *trans*- and *cis*-isomers of Flupentixol. The largest IR intensity of the two spectra is related to the C8-H31, C9-H34, C10-H35, C11-H38, and C13-H41 stretching vibrations. Their corresponding frequencies are observed at 2918 and 2917 cm^{-1} for the *trans*- and *cis*-structures, respectively. For the CF_3 group, the stretching vibrations are reported in the ranges 1045–1083 and 1045–1098 cm^{-1} for the *trans*- and *cis*-structures, respectively. For the *trans*- and *cis*-structures of Flupentixol, the OH vibration modes are observed at 287 and 289 cm^{-1}, respectively. We can find that the IR intensities of the *cis*-structure are slightly larger than those of the *trans*-structure, which can explain the better properties of *cis*-Flupentixol as a drug.

TABLE 5. Selected Vibrational Frequencies (ν, cm^{-1}), IR Intensities (I_{IR}, km/mole), and Assignment for the *trans*- and *cis*-Isomers of Flupentixol Calculated at the B3LYP/6-311+G** Level in Water

ν	I_{IR}	Obvious assignment
trans-Flupentixol		
2918	635	C8-H31, C9-H34, C10-H35, C11-H38 and C13-H41 stretching
1274	346	C24-C30 stretching, C22-H48 and C25-H51 bending
1083	297	C-C stretching and bending in the rings of the molecule, C30-F3 streching
1045	416	C30-F2, C30-F3 and C30-F4 stretching
287	91	Torsional O5-H50 vibration
cis-Flupentixol		
2917	651	C8-H31, C9-H34, C10-H35, C11-H38 and C13-H41 stretching
1278	399	C24-C30 stretching, C22-H48 and C25-H51 bending
1098	285	C-C stretching and bending in entire of the molecule, C30-F2 streching
1045	411	C30-F2, C30-F3 and C30-F4 stretching
289	111	Torsional O5-H50 vibration

TABLE 6. Thermodynamic Properties at Different Temperatures of the *trans*- and *cis*-Structures of Flupentixol, at the B3LYP/6-311+G** Level in Water

T, K	E_0	*E*	*C*	*S*	Δ*H*
trans-Flupentixol					
100	277.8	280.4	42.5	112.9	280.5
200	277.8	286.2	73.7	153.3	286.5
273	277.8	292.4	97.5	180.3	292.9
298.15	277.8	295.0	105.8	189.5	295.5
300	277.8	295.2	106.4	190.1	295.7
400	277.8	307.5	138.5	225.8	308.2
500	277.8	322.7	166.2	260.2	323.7
cis-Flupentixol					
100	277.8	280.4	42.6	112.3	280.5
200	277.8	286.2	73.7	152.7	286.5
273	277.8	292.4	97.5	179.8	292.9
298.15	277.8	294.9	105.9	188.9	295.5
300	277.8	295.2	106.5	189.6	295.7
400	277.8	307.5	138.5	225.2	308.2
500	277.8	322.7	166.2	259.7	323.7

Thermodynamic properties. The thermodynamic parameters of the *trans*- and *cis*-structures were calculated for different temperatures from 100 to 500 K by the B3LYP/6-311+G** method in water solvent and are listed in Table 6. According to Table 6, the thermodynamic parameters of the *trans*- and *cis*-isomers of Flupentixol are almost close to each other. The zero-point vibrational energies, total thermal energies, entro-

py, and enthalpy changes of the *trans*-structure of Flupentixol are less than those of the *cis*-structure, while the heat capacities of *cis*-Flupentixol is less than those of *trans*-Flupentixol. Also, these results show that all the thermodynamic qualities, except for the zero-point vibrational energy, are increasing with increasing temperature from 100 to 500 K, because the molecular vibrational intensities improve with temperature while the zero-point vibrational energy does not change with temperature [41, 46].

Conclusion. The geometries, electronic properties, electronic absorption spectra, nonlinear optical properties, thermodynamic properties, natural charge distribution, MEP analysis, and vibrational frequencies of the *trans*- and *cis*-structures of Flupentixol were studied by DFT methods to compare the *trans*- and *cis*-structures of Flupentixol and to explain why its *cis*-structure can act as a drug. All quantum parameters confirm the better activity of the *cis*-structure.

REFERENCES

1. A. G. Goodman, L. S. Gilman, *The Pharmacological Basis of Therapeutics*, **1**, 8th ed., Pergamon Press, New York (1995).
2. S. Ruhrmann, W. Kissling, O.M. Lesch, M. Schmauss, U. Seemann, M. Philipp, *Prog. Neuro-Psychopharmacol. Biol. Psychiatry*, **31**, 1012–1022 (2007).
3. S. Walter, S. Bauer, I. Roots, J. Brockmoller, *J. Chromatogr. B*, **720**, 231–237 (1998).
4. A. A. Elbary, A. A. Ramadan, I. R. Bendas, D. A. E. Mostafa, *Int. Res. J. Pharm*., **2**, No. 9, 58–64 (2011).
5. Z. Talebpour, S. Haghgoo, M. Shamsipur, *Anal. Biochem*., **323**, 205–210 (2003).
6. S. Ulrich, *J. Chromatogr. B*, **668**, 31–40 (1995).
7. D. Yonara, M. M. Sunnetcioglu, *Chem. Phys. Lipids*, **198**, 61–71 (2016).
8. V. Markovic, M. D. Joksovic, S.Markovic, I. Jakovljevic, *J. Mol. Struct*., **1058**, 291–297 (2014).
9. G. M. J. Beijersbergen van Henegouwen, *Adv. Drug. Res*., **29**, 79–170 (1997).
10. A. A. Kaczor, K. M. Targowska-Duda, B. Budzyńska, G. Biała, A. G. Silva, M. Castro, *Neurochem. Int*., **96**, 84–99 (2016).
11. V. Krishnakumar, K. Murugeswari, N. Surumbarkuzhali, *Spectrochim. Acta A: Mol. Biomol. Spectrosc*., **114**, 410–420 (2013).
12. Ö. Bağlayan, M. Fatih Kaya, E. Güneş, M. Şenyel, *J. Mol. Struct*., **1122**, 324–330 (2016).
13. G. Mahalakshmi, V. Balachandran, *Spectrochim. Acta A: Mol. Biomol. Spectrosc*., **131**, 587–598 (2014)
14. P. Rajesh, S. Gunasekaran, T. Gnanasambandan, S. Seshadri, *Spectrochim. Acta A: Mol. Biomol. Spectrosc*., **137**, 1184–1193 (2015).
15. J. L. Waddington, S. J. Gamble, R. C. Bourne, *Eur. J. Pharmacol*., **69**, 511–513 (1981).
16. J. Kim, J. H. Song, *Eur. J. Pharmacol*., **779**, 31–37 (2016).
17. I. Pajeva, D. K. Todorov, J. Seydel, *Eur. J. Pharm. Sci*., **21**, 243–250 (2004).
18. T. Sokoließ, U. Menyes, U. Roth, T. Jira, *J. Chromatogr. A*, **948**, 309–319 (2002).
19. M. W. Schmidt, K. K. Baldridge, J. A. Boatz, S. T. Elbert, M. S. Gordon, J. H. Jensen, S. Koseki, N. Matsunaga, K. A. Nguyen, S. Su, T. L. Windus, M. Dupuis, J. John, A. Montgomery, *J. Comput. Chem*., **14**, 1347–1363 (1993).
20. M. Cossi, N. Rega, G. Scalmani, V. Barone, *J. Comput. Chem*., **24**, 669–681 (2003).
21. M. Cossi, V. Barone, R. Cammi, J. Tomasi, *Chem. Phys. Lett*., **255**, 327–335 (1996).
22. V. Barone, M. Cossi, *J. Phys. Chem. A*, **102**, 1995–2001 (1998).
23. P. Hohenberg, W. Kohn, *Phys. Rev*., **136B**, 864–871 (1964).
24. C. T. Lee, W. T. Yang, R. G. Parr, *Phys. Rev*., **37B**, 785–789 (1988).
25. R. G. Parr, W. Yang, *Ann. Rev. Phys. Chem*., **46**, 701–728 (1995).
26. A. D. Becke, *J. Chem. Phys*., **98**, 5648–5652 (1993).
27. S. Bagheri Novir, S. M. Hashemianzadeh, *Mol. Phys*., **114**, 650–662 (2016).
28. S. Bagheri Novir, S. M. Hashemianzadeh, *Spectrochim. Acta A: Mol. Biomol. Spectrosc.*, **143**, 20–34 (2015).
29. C. R. Zhang, L. Liu, Z. J. Liu, Y. L. Shen, Y. T. Sun, Y. Z. Wu, Y. H. Chen, L. H. Yuan, W. Wang, H. S. Chen, *J. Mol. Graph. Model*., **38**, 419–429 (2012).
30. C. R. Zhang, Z. J. Liu, Y. H. Chen, H. S. Chen, Y. Z. Wu, L. H. Yuan, *J. Mol. Struct. (THEOCHEM)*, **899**, 86–93 (2009).
31. P. S. Kumar, K. Vasudevan, A. Prakasam, M. Geetha, P. M. Anbarasan, *Spectrochim. Acta A: Mol. Biomol. Spectrosc.*, **77**, 45–50 (2010).

32. S. Xavier, S. Periandy, S. Ramalingam, *Spectrochim. Acta A: Mol. Biomol. Spectrosc*., **137**, 306–320 (2015).
33. Y. J. Jiang, Z. Liu, H. Liu, W. Y. Cui, N. Wang, D. Liu, X. W. Ge, *Chin. Sci. Bull*., **57**, No. 34, 4448–4452 (2012).
34. L. Sinha, M. Karabacak, V. Narayan, M. Cinar, O. Prasad, *Spectrochim. Acta A: Mol. Biomol. Spectrosc.*, **109**, 298–307 (2013).
35. N. R. Sheela, S. Muthu, S. Sampathkrishnan, *Spectrochim. Acta A: Mol. Biomol. Spectrosc.*, **120**, 237–251 (2014).
36. T. A. Koopmans, *Physica*, **1**, 104–113 (1934).
37. R. G. Pearson, *J. Am. Chem. Soc*., **85**, 3533–3539 (1963).
38. X. Zarate, E. Schott, T. Gomez, R. Arratia-Perez, *J. Phys. Chem. A*, **117**, 430–438 (2013).
39. R. G. Parr, R. A. Donnelly, M. Levy, W. E. Palke, *J. Chem. Phys*., **68**, 3801–3807 (1978).
40. A. Srivastava, P. Rawat, P. Tandon, R. N. Singh, *Comput. Theor. Chem*., **993**, 80–89 (2012).
41. V. Balachandran, S. Rajeswari, S. Lalitha, *Spectrochim. Acta A: Mol. Biomol. Spectrosc.*, **124**, 277–284 (2014).
42. R. G. Parr, L.V. Szentpaly, S. Liu, *J. Am. Chem. Soc*., **121**, 1922–1924 (1999).
43. H. Tanak, M. Toy, *J. Mol. Struct*., **1068**, 189–197 (2014).
44. Y. Shyma Mary, P. J. Jojo, C. Van Alsenoy, M. Kaur, M. S. Siddegowda, H. S. Yathirajan, H. I. S. Nogueira, S. M. A. Cruz, *Spectrochim. Acta A: Mol. Biomol. Spectrosc.*, **120**, 370–380 (2014).
45. P. Politzer, P. R. Laurence, K. Jayasuriya, *Health Persp*., **61**, 191–202 (1985).
46. J. Bevan Ott, J. Boerio-Goates, *Calculations from Statistical Thermodynamics*, Academic Press (2000).